The Plant Cell, Vol. 8, 859–871, May 1996

Two Small Spatially Distinct Regions of Phytochrome B Are Required for Efficient Signaling Rates

Doris Wagner,[a,b,1] Michael Koloszvari,[a,b] and Peter H. Quail[a,b,2]

[a] Department of Plant Biology, University of California–Berkeley, Berkeley, California 94720
[b] Plant Gene Expression Center, U.S. Department of Agriculture, 800 Buchanan Street, Albany, California 94710

We used a series of in vitro-generated deletion and amino acid substitution derivatives of phytochrome B (phyB) expressed in transgenic Arabidopsis to identify regions of the molecule important for biological activity. Expression of the chromophore-bearing N-terminal domain of phyB alone resulted in a fully photoactive, monomeric molecule lacking normal regulatory activity. Expression of the C-terminal domain alone resulted in a photoinactive, dimeric molecule, also lacking normal activity. Thus, both domains are necessary, but neither is sufficient for phyB activity. Deletion of a small region on each major domain (residues 6 to 57 and 652 to 712, respectively) was shown to compromise phyB activity differentially without interfering with spectral activity or dimerization. Deletion of residues 6 to 57 caused a large increase in the fluence rate of continuous red light (Rc) required for maximal seedling responsiveness, indicating a marked decrease in efficiency of light signal perception or processing per mole of mutant phyB. In contrast, deletion of residues 652 to 712 resulted in a photoreceptor that retained saturation of seedling responsiveness to Rc at low fluence rates but at a response level much below the maximal response elicited by the parent molecule. This deletion apparently reduces the maximal biological activity per mole of phyB without a major decrease in efficiency of signal perception, thus suggesting disruption of a process downstream of signal perception. In addition, certain phyB constructs caused dominant negative interference with endogenous phyA activity in continuous far-red light, suggesting that the two photoreceptors may share reaction partners.

INTRODUCTION

Phytochromes are the best characterized of the photoreceptors that control many aspects of early seedling development. These molecules are dimers with a monomeric molecular mass of ~125 kD. Each monomer consists of two major structural domains: a chromophore-bearing, globular N-terminal domain (Vierstra and Quail, 1986) and an extended C-terminal domain, which carries the dimerization sites (Jones et al., 1986; Vierstra et al., 1987; Edgerton and Jones, 1992; Cherry et al., 1993).

In Arabidopsis, the phytochromes are encoded by five different genes—*PHYA* through *PHYE* (Sharrock and Quail, 1989; Clack et al., 1994). Contrasting photosensory functions of the phyA and phyB holoproteins have been defined through analysis of responses to constitutive overexpression of (Boylan and Quail, 1989, 1991; Kay et al., 1989; Keller et al., 1989; Cherry et al., 1991; Wagner et al., 1991; McCormac et al., 1993) and mutations in (Nagatani et al., 1991, 1993; Somers et al., 1991; Dehesh et al., 1993; Parks and Quail, 1993; Reed et al., 1993; Whitelam et al., 1993; Wagner and Quail, 1995; Xu et al., 1995) both sequences. phyA controls deetiolation (inhibition of hypocotyl elongation, hook opening, and cotyledon expansion) in continuous far-red light (FRc), whereas phyB is primarily responsible for deetiolation in continuous red light (Rc). phyA is most abundant in dark-grown seedlings (~50-fold phyB levels), whereas, due to light-induced phyA degradation, phyB is more abundant in Rc (approximately twofold phyA) (Somers et al., 1991; Quail, 1994). The function of phyC, phyD, and phyE remains unclear.

The molecular mechanism of action of neither phyA nor phyB is understood. In attempts to identify functionally important structural domains of oat phyA, several researchers have analyzed the effect of in vitro–generated deletion and amino acid substitution mutants on the ability of the photoreceptor to cause increased inhibition of hypocotyl or stem elongation when overexpressed in transgenic Arabidopsis or tobacco, respectively (Cherry et al., 1992, 1993; Stockhaus et al., 1992; Boylan et al., 1994). Taken together, these data indicate that the N-terminal domain is sufficient for spectral integrity but not for normal biological activity of the protein and that regions at the N and C termini of phyA are necessary for normal biological activity. Some differences were observed in the biological activity of similar constructs between tobacco and Arabidopsis, but the reasons for this observation are not understood (Cherry et al., 1992; Boylan et al., 1994).

[1] Current address: Division of Biology 156-29, California Institute of Technology, Pasadena, CA 91125.
[2] To whom correspondence should be addressed.

No such structure–function analysis has been reported for phyB, which shares 50% amino acid identity with phyA (Sharrock and Quail, 1989; Dehesh et al., 1991). Accumulating evidence suggests that differential photosensory specificity is due directly to the differences in primary structure of phyA and phyB rather than to differential expression of the two photoreceptors (Somers and Quail, 1995; Wagner et al., 1996). Thus, structural analysis of phyB may identify elements required specifically for phyB activity and/or regions required for activity of both photoreceptors. Here, we have used overexpression of a series of site-directed mutants of phyB in transgenic Arabidopsis to approach this question.

RESULTS

phyB Deletion and Amino Acid Substitution Derivatives Are Overexpressed at High Levels

To analyze the functional importance of structural domains of Arabidopsis phyB, we generated seven different deletion derivatives and one point mutation derivative of phyB, as shown in Figure 1. All constructs share the first five amino acids of phyB (small black boxes). The phyB/phyD group of phytochromes carries a 10- to 37-amino acid N-terminal extension, which is not found in the other phytochromes (Clack et al., 1994). Four N-terminal deletions were constructed to test (1) the importance of this N-terminal extension (ΔN57, lacking amino acids 6 to 57); (2) the function of additional N-terminal regions, which were shown to be important for phyA activity (Cherry et al., 1992; Boylan et al., 1994) (ΔN90 and ΔN103, lacking amino acids 6 to 90 and amino acids 6 to 103, respectively); and (3) the biological activity of the C-terminal domain when overexpressed by itself (ΔN633, which lacks amino acids 6 to 633). All four constructs can be detected immunochemically with a monoclonal antibody (MAb B2), which recognizes an epitope between amino acids 652 and 712 of phyB. (Epitope analysis is described in Methods.) The C357-S phyB derivative carries a single amino acid change, which converts the chromophore attachment site at cysteine 357 to serine. The resulting molecule is predicted to be spectrally inactive, as is phyA carrying this mutation (Boylan et al., 1994), because the thiol group involved in covalent chromophore attachment is changed to an inactive hydroxyl group.

Two additional constructs were designed to test the functional importance in phyB of putative dimerization sites reported for phyA (Edgerton and Jones, 1992, 1993). Δ652-712 (lacking amino acids 652 to 712) removes the phyB equivalent of the putative central dimerization site and ΔC1087 (lacking amino acids 1087 to 1172) of the putative C-terminal dimerization site reported for phyA. Finally, Δ652 (which lacks amino acids 652 to 1172) is the reciprocal deletion to ΔN633 (above) and tests the activity of the globular, chromophore-bearing N-terminal domain, when overexpressed by itself.

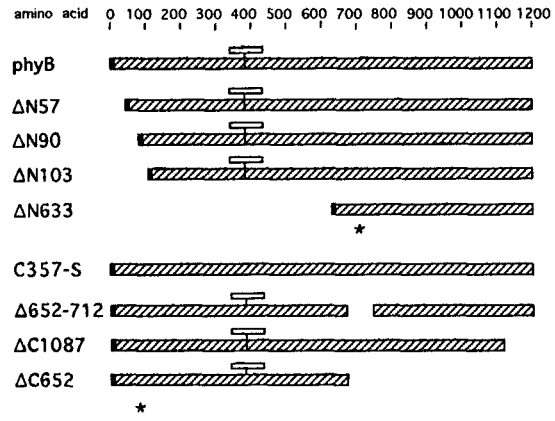

Figure 1. Schematic of phyB-Derivative Constructs Used for Arabidopsis Transformation.

Full-length phyB (top) and eight phyB-derivative constructs used for transformation and phenotypic analysis in Arabidopsis are shown drawn to scale (hatched boxes). The name of each construct is indicated at left. Amino acids are numbered above. All constructs are deletion derivatives except C357-S, which carries a single amino acid change (cysteine 357 is mutated to serine). The small, filled boxes at the N termini indicate the first five amino acids of phyB that are retained in all constructs. The open boxes above the constructs represent the linear tetrapyrrole chromophore. The asterisks below ΔN633 and ΔC652 indicate the positions of epitopes recognized by two MAbs (MAb B2 and MAb B1, respectively) used for immunochemical detection of the polypeptides.

For immunochemical detection of constructs C357-S through ΔC652, a second MAb (MAb B1) was used, which recognizes an epitope on phyB, overlapping with amino acids 90 to 103. All constructs (including phyB) were transformed into Arabidopsis (ecotype NO-O), using the vector described by Wagner et al. (1991), so that each was comparable to the reference phyB overexpressing line ABO (Wagner et al., 1991). At least 50 independent transgenic lines were generated per construct, and after testing for the transformation marker, the level of overexpression was analyzed immunochemically in each line.

To enable determination of the biological activity of the phyB derivatives, the expression level of each construct should be comparable to that found in the ABO reference line overexpressing unmutagenized phyB. Figure 2 shows the hypocotyl length of at least five independent transformants for each construct in Rc (22.0 μmol m^{-2} sec^{-1}) as a function of the amount of phyB or phyB derivative overexpressed compared with ABO and the untransformed control (NO-O). The amount of the transgene expression was either determined spectrophotometrically (ΔΔA; Figures 2A to 2F) or densitometrically from immunoblots for ΔN633 and C357-S, which were spectrally inactive (Figures 2G and 2H). We were able to identify transgenic lines that showed overexpression comparable to that seen in ABO for all phyB derivatives except ΔC1087. This construct was expressed at very low levels in at least 60 independent transgenic

lines, suggesting that this deletion renders the resulting polypeptide (or mRNA) unstable (data not shown). For all other constructs, the transgenic lines chosen for further analyses, based on an overexpression level similar to that of phyB in the ABO line, are indicated in Figure 2.

Analysis of hypocotyl elongation of transgenic lines that overexpress Arabidopsis phyB at different levels showed that overexpression levels of approximately three- to fourfold that of endogenous phyB already resulted in the full inhibition of hypocotyl elongation (saturation of the response; Figure 2A). By comparison, the Δ652-712 lines appeared to be partially active because hypocotyl elongation was reduced as compared with NO-O, but not as much as in seedlings overexpressing phyB at similar levels (Figure 2B). ΔC652 (Figure 2C) appeared to be biologically inactive (the hypocotyl length was equal to that of NO-O) over a wide range of expression levels. At the highest level of overexpression (~100-fold that of the endogenous phyB level), hypocotyl elongation appeared slightly enhanced in ΔC652 as compared with NO-O. Deletion of the N-terminal phyB/phyD–specific extension (ΔN57) resulted in an almost fully active polypeptide (Figure 2D) over a range of expression levels when compared with lines overexpressing phyB. A slight loss of activity was apparent for ΔN57 at lower levels of expression under the conditions used here. More extensive deletion of N-terminal regions (ΔN90 and ΔN103; Figures 2E and 2F) resulted in a significant reduction of biological activity as compared with phyB or ΔN57. Neither of the spectrally inactive constructs (C357-S or ΔN633; Figures 2G and 2H) were biologically active over the range of expression levels analyzed.

Figure 3 shows the immunochemically detectable amount of overexpressed phyB in the lines chosen for further study (Figure 2) as well as in the highest level ΔC1087 overexpressing line. Two different MAbs (recognizing epitopes on either the N-terminal [MAb B1] or the C-terminal [MAb B2] domain) were used as probes, and levels of phyB derivatives were compared with the untransformed NO-O and ABO lines included on both blots. Figure 3A shows that all N-terminal deletions were expressed at levels equivalent to that of phyB in ABO. Endogenous phyB could be observed faintly in NO-O as well as in the deletion constructs. The amount of spectrally active protein in each line is shown below the blot (Figure 3C) and was found to parallel the immunoblot data, except for the spectrally inactive ΔN633 protein. However, the amount of phyB in this line, as determined by densitometry, was equal to that in ABO (Figure 3C). Figure 3B shows that the level of expression in Δ652-712 was approximately equal to that of phyB in ABO, whereas C357-S and ΔC652 were expressed at slightly higher levels and ΔC1087 at much lower levels. The ΔΔA data paralleled the immunoblot data, except for the spectrally inactive C357-S construct, in which the densitometrically determined phyB levels agreed with the visualization of the immunoblot data (Figure 3C). The apparent slightly weaker signals in ΔN633 and ΔC652 were due to their position at the bottom of the gel and were not observed when higher percentage gels were probed. The molecular masses of all deletion constructs were similar to the expected size (data not shown). Some smaller products could be observed in the ABO, ΔN57, and C357-S lanes. These are most likely degradation products generated postextraction (data not shown).

Most phyB Deletion Derivatives Are Dimeric and Have Unaltered Difference Spectra

To assess the gross structural integrity of the phyB derivatives, we tested their dimerization capabilities, using nondenaturing gradient gel electrophoresis. The extracts used for Figure 3 were subjected to high-speed centrifugation (400,000*g*) and analyzed by electrophoresis on 4 to 30% nondenaturing gels, as shown in Figure 4. Overexpressed phyB was dimeric under these conditions (Figures 4A and 4B, lanes 2) as is endogenous phyB (Wagner and Quail, 1995). phyB dimers migrated at 317 kD, slightly smaller than the apparent molecular mass of phyA (347 kD). As expected, the small N-terminal deletions (ΔN57, ΔN90, and ΔN103) also appeared to migrate as dimers, with slightly increased mobility as compared with ABO (Figure 4A).

ΔN633 migrated approximately three times slower (174 kD) than predicted from its monomeric molecular mass and therefore appeared to be dimerization competent. Data similar to these for phyA have been interpreted as indicative of dimeric entities, which migrate more slowly than expected because the C-terminal domain of phytochrome has an extended conformation (Quail, 1991). In addition, C357-S and Δ652-712 appeared dimeric by this analysis when compared with ABO (Figure 4B). Thus, it appears that the region between amino acids 652 and 712, which corresponds to a putative dimerization site of phyA (Edgerton and Jones, 1992, 1993), is not necessary for phyB dimerization. This suggests that for phyB, the equivalent of the second, C-terminal dimerization site of phyA (residues 1049 to 1094) (Edgerton and Jones, 1992; Cherry et al., 1993) may be sufficient by itself for dimerization. However, the amount of Δ652-712 visualized was reduced as compared with the denaturing electrophoresis (Figure 3). No other band was seen in the Δ652-712 lane. Because the same extracts were used for both types of gels, one possibility to explain the loss in the Δ652-712 signal is that some of this derivative polypeptide was lost (pelleted) during the high-speed centrifugation before the native electrophoresis. ΔC652 migrated close to its monomeric position on nondenaturing gel electrophoresis (Figure 4B). A slightly higher molecular mass band observed in lane 6 of Figure 4B was apparently aberrant because it was not seen in repeat experiments. The levels of ΔC1087 are too low for interpretation.

Only a single band was observed in the ΔN633 extracts (Figure 4A), which could be the result of homomeric complexes of ΔN633. Alternatively, all ΔN633 could be in heteromeric complexes with endogenous phyB. To distinguish between these two possibilities, we subjected ΔN633 and NO-O to native

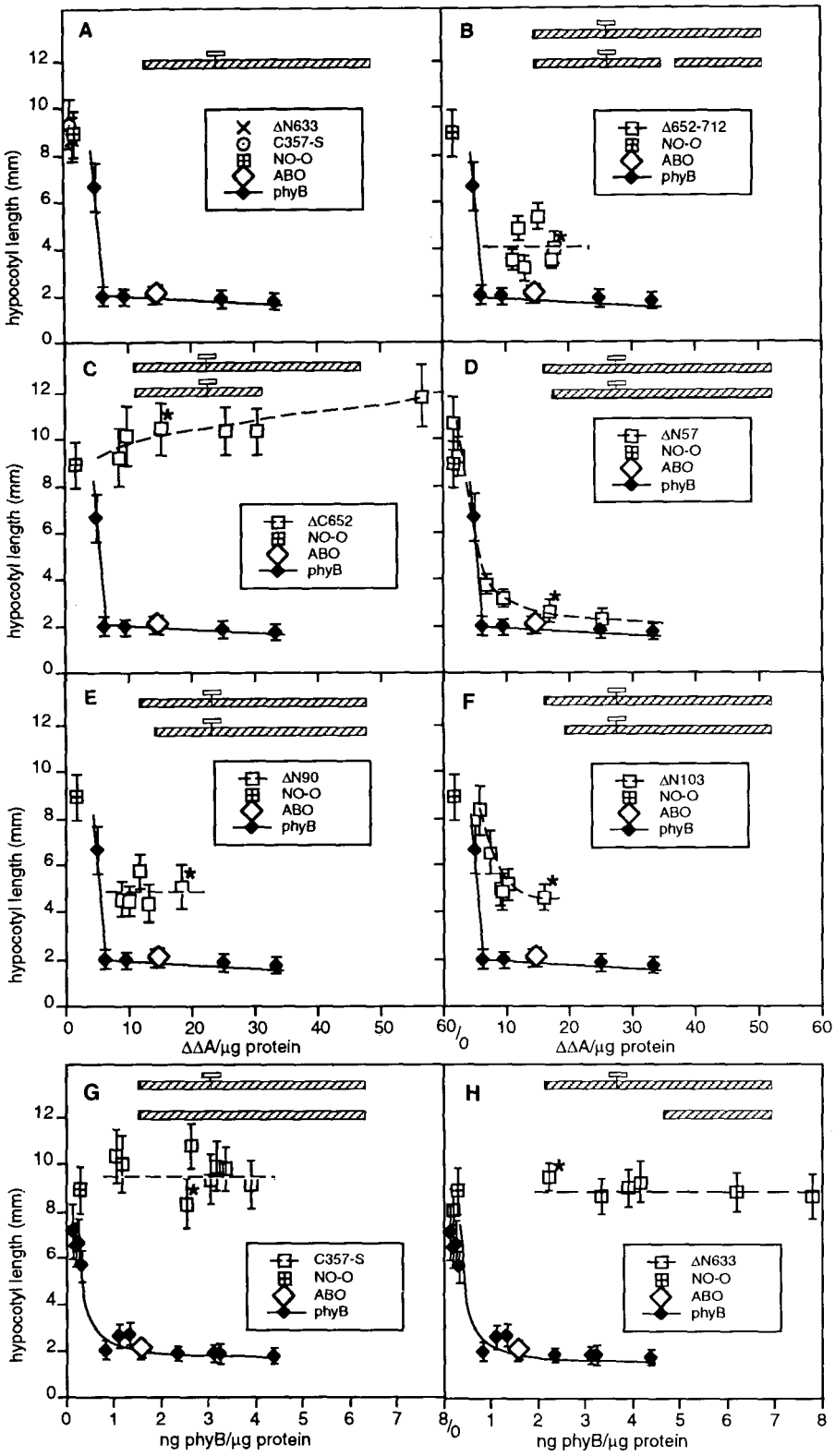

Figure 2. Hypocotyl Length as a Function of the Level of Overexpression of phyB and of the Mutant phyB Derivatives in Rc (22 μmol m^{-2} sec^{-1}).

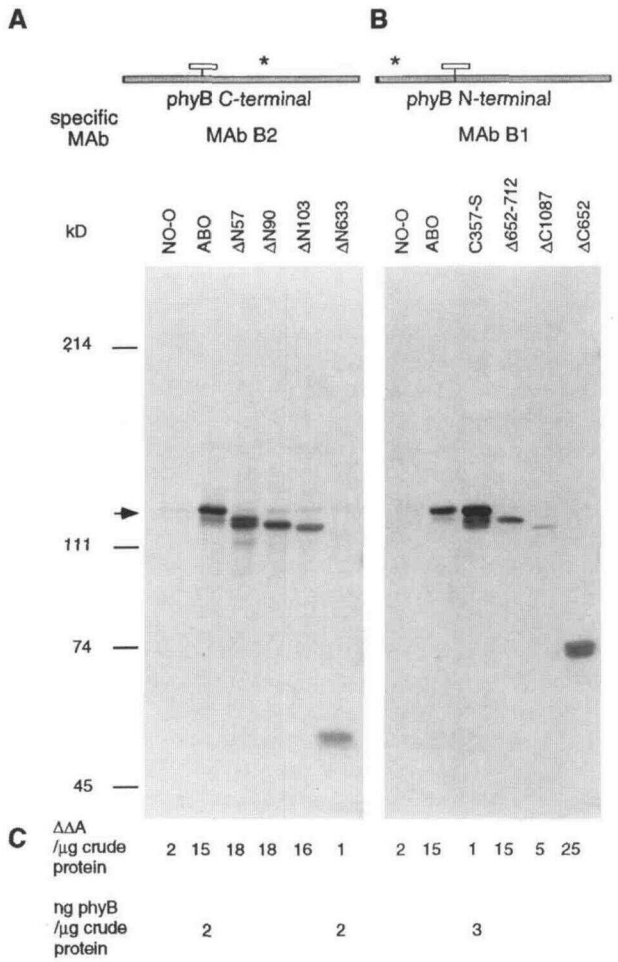

Figure 3. Levels of phyB and phyB Mutant Derivatives Overexpressed in Selected Lines.

electrophoresis and probed the right half of the immunoblot with MAb B2, which recognizes ΔN633 and endogenous phyB, whereas the left half was probed with MAb B1, which only recognizes endogenous phyB (Figure 4C). Based on analysis of the expression of phyB and 35S promoters (Somers and Quail, 1995), at least some of the constitutively expressed ΔN633 should be present in the same cells as endogenous phyB. However, no endogenous phyB was detectable in the 174-kD band when analyzed with MAb B1 (Figure 4C, left). In addition, with neither MAb was a significant reduction of endogenous phyB levels at 317 kD observed in the ΔN633 lanes compared with the NO-O lanes, suggesting that the 174-kD band consists of ΔN633 homomeric complexes alone.

Figure 4D further supports the conclusion that the 174-kD band in ΔN633 plants represents homomeric ΔN633 complexes. We analyzed NO-O, a *phyB* null mutant (derived from *phyB-1*), ΔN633, and ΔN633 in the homozygous *phyB-1* background by native electrophoresis. The 174-kD band was present at equal levels in the *phyB* null mutant and NO-O (wild type)

Shown are immunochemical, spectral, and densitometric determinations of phyB levels in the extracts of all lines chosen (as given in Figure 2). Epitopes recognized by MAb B2 (between amino acids 652 to 712) and MAb B1 (near amino acids 90 to 103) are indicated with asterisks above the diagram.

(A) Immunoblot probed with MAb B2.

(B) Immunoblot probed with MAb B1.

(C) Amount of overexpressed phyB or phyB derivative in each line as determined by spectral (ΔΔA/μg of crude protein) or densitometric (ng of phyB/μg of crude protein) analysis.

(A) and **(B)** show crude extracts of 7-day-old Rc-grown seedlings that were subjected to denaturing gel electrophoresis (6.5%) and immunoblotting. Sixty micrograms of crude protein was loaded per lane. The line names (constructs are given in Figure 1) are indicated above each lane; the untransformed wild-type extract lane is to the left (NO-O). Molecular mass markers are indicated to the left (in kilodaltons). The arrow points to full-length phyB (122 kD).

Figure 2. (continued).

Phytochrome levels were measured by ΔΔA analysis (**[A]** to **[F]**) and by densitometric analysis of immunoblots (**[G]** and **[H]**). A schematic of the construct analyzed is shown at top in **(A)** to **(H)**.

(A) Transgenic phyB seedlings.

(B) Transgenic Δ652-712 seedlings.

(C) Transgenic ΔC652 seedlings.

(D) Transgenic ΔN57 seedlings.

(E) Transgenic ΔN90 seedlings.

(F) Transgenic ΔN103 seedlings.

(G) Transgenic C357-S seedlings.

(H) Transgenic ΔN633 seedlings.

In **(A)**, the hypocotyl lengths of the untransformed wild-type NO-O, the reference phyB overexpressing line ABO, and a series of plants overexpressing phyB at different levels as well as one line each of the spectrally inactive ΔN633 and C357-S transformants are shown. In **(B)** to **(H)**, the hypocotyl lengths of the seedlings containing the construct analyzed are compared with those of the untransformed wild-type NO-O, the reference phyB overexpressing line ABO, and a series of plants overexpressing phyB at different levels. The lines chosen for further analysis that have similar overexpression levels as found in ABO are marked by an asterisk.

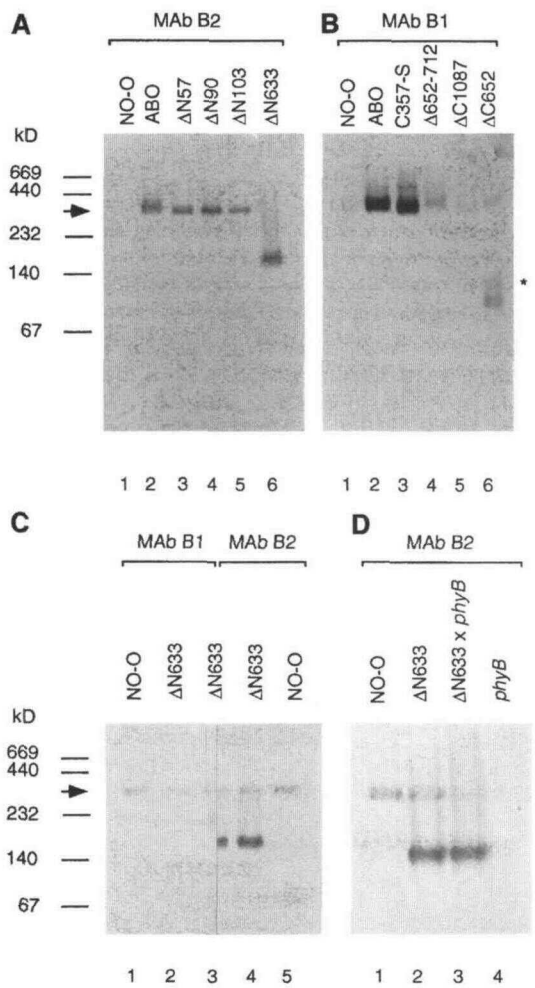

Figure 4. Nondenaturing Gel Electrophoresis and Immunoblot Analysis of phyB and Derivative Constructs.

(A) Native molecular mass of phyB derivatives determined on an immunoblot probed with MAb B2.

(B) Native molecular mass of phyB derivatives determined on an immunoblot probed with MAb B1.

(C) Native molecular mass of ΔN633 determined on immunoblots probed with MAb B1 and MAb B2.

(D) Native molecular mass of ΔN633 in NO-O and in the *phyB-1* (null) backgrounds determined on immunoblots probed with MAb B2.

MAb B2 and MAb B1 are as described in Figure 3. Molecular mass of nonstained markers is indicated on the left (kD). The arrows point to full-length phyB (317 kD).

(A) and **(B)** show nondenaturing gel electrophoresis of the extracts used for Figure 3. After centrifugation at 400,000*g*, the extracts used for Figure 3 were subjected to native gradient gel electrophoresis (4 to 30%), and 80 μg of crude protein was loaded per lane. The order of lanes is as given in Figure 3. The asterisk at right of ΔC652 **(B)** denotes an upper band that was not apparent in repeat experiments. In **(C)**, crude extracts were prepared from 7-day-old etiolated seedlings, and 14 μg of crude protein was loaded per lane. Three lanes of ΔN633 (lanes 2 to 4) are flanked by two lanes of untransformed NO-O (lanes 1 and 5). Lane 3 is cut in half vertically. The left half of the blot was probed with MAb B1, which recognizes endogenous phyB under these staining conditions, whereas the right half was developed with MAb B2, which recognizes both endogenous phyB and ΔN633. In **(D)**, extracts were prepared and loaded as described for **(C)**. Native gel electrophoresis of extracts derived from NO-O, ΔN633, the *phyB-1* null mutant, and from a line homozygous for both ΔN633 and the *phyB-1* mutation was performed, and the immunoblot was developed with MAb B2.

backgrounds, indicating that endogenous phyB is not an integral component of the transgene-encoded high molecular mass species.

In Figure 5, the spectral properties of all phyB derivatives were compared with phyB by difference spectrum analysis, which is a sensitive indicator of the integrity of those parts of the polypeptide involved in chromophore interaction. No difference spectra could be observed in NO-O or in the spectrally inactive C357-S and ΔN633 lines because the level of endogenous phytochromes was too low for detection in Rc grown tissue under these analytic conditions. All other phyB derivatives showed difference spectra that were very similar to that seen in ABO, indicating that all spectrally active phyB derivatives are spectrally normal. In addition, as for phyA, the N-terminal domain of phyB is sufficient for spectral integrity. Due to the small signal in some of the lines, exact determination of the position of maxima and minima was difficult. The small N-terminal deletion constructs appeared to show a slightly blue-shifted minimum, as had been found for similar deletion constructs of phyA (Cherry et al., 1992; Boylan et al., 1994).

The N Terminus of phyB and a Small Central Region Are Important for Normal phyB Activity

To analyze more quantitatively the extent of loss of biological activity, all transgenic lines expressing phyB and phyB derivatives as well as NO-O (wild type) were grown under two fluence rates of red light (22.0 μmol m^{-2} sec^{-1} and 0.1 μmol m^{-2} sec^{-1}), as shown in Figure 6A. At 22.0 μmol m^{-2} sec^{-1}, we again observed almost full activity of ΔN57 and partial activity of ΔN90, ΔN103, and Δ652-712 as compared with ABO and the untransformed NO-O control, whereas ΔN633, C357-S, ΔC1087, and ΔC652 were inactive (also shown in Figure 2). However, at 0.1 μmol m^{-2} sec^{-1} of Rc, it was apparent that all three small N-terminal deletion constructs (ΔN57, ΔN90, and ΔN103) were biologically inactive: hypocotyl length was indistinguishable from that of seedlings of the same line grown in the dark. Similarly, NO-O, C357-S, ΔN633, and ΔC652 showed hypocotyl lengths indistinguishable from those of the dark controls, whereas ABO and Δ652-712 were much shorter in 0.1 μmol m^{-2} sec^{-1} Rc than in darkness.

To provide a more comprehensive quantitative analysis, we further investigated hypocotyl elongation over a range of Rc fluence rates for all transgenic lines carrying biologically active transgenes as well as for ABO and NO-O (Figure 6B). The

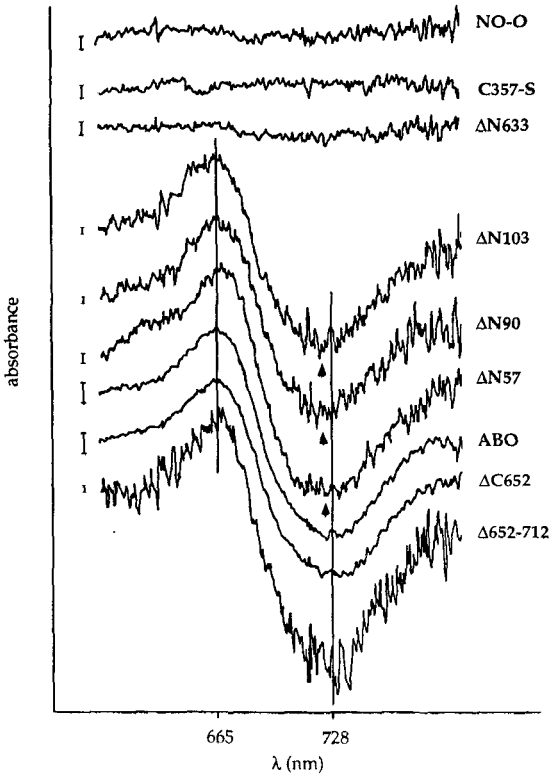

Figure 5. Difference Spectra of phyB and phyB Mutant Derivatives.

Extracts concentrated 26- to 36-fold with ammonium sulfate were generated from 7-day-old transgenic seedlings overexpressing phyB and phyB mutant derivatives grown in Rc. Extracts were subjected to difference spectrum analysis without adjusting for equal crude protein concentration. The names of the constructs are at right. The position of the maxima and minima of phyB are indicated by vertical lines at 665 and 728 nm, respectively. Arrowheads point to the position of the blue-shifted minima in the lines carrying small N-terminal deletions. The bar to the left of each spectrum indicates 10^{-3} absorbance units.

N-terminal deletion constructs were almost fully active in high fluence rates of Rc when compared with ABO but showed markedly decreased activity in lower fluence rates relative to ABO. The data suggest that the small N-terminal deletion constructs require higher fluence rates of Rc for activity than does phyB, indicating that these molecules are less sensitive to Rc on a per mole basis but do not reduce maximal possible signal throughput (capacity) at high fluence rate Rc. Surprisingly, Δ652-712, which showed only weak activity at 22.0 μmol m^{-2} sec^{-1} Rc, exhibited saturation of the response at 0.1 μmol m^{-2} sec^{-1} Rc. Thus, this deletion appears to not reduce the per mole quantum efficiency but to cause a reduction in the maximal signal throughput (capacity) of the molecule. All lines had hypocotyl lengths similar to that of NO-O in the dark, indicating that the phenotypes observed are red-light dependent and therefore most likely due to the activity of the transgenes and not to random transformation effects.

Overexpression of phyB, ΔN633, or ΔC652 Interferes with Endogenous phyA Activity

When we analyzed the effect of overexpression of phyB and the phyB deletion derivatives on hypocotyl elongation in FRc, we observed dominant negative interference (Herskowitz, 1987) of phyB, ΔN633, and ΔC652 with endogenous phyA activity, as shown in Figure 7. When compared with the effect of Rc on hypocotyl elongation (as in Figure 2), an interesting picture emerged. Increasing phyB levels caused an increasing dominant negative interference in FRc compared with NO-O, whereas it resulted in increasing inhibition of hypocotyl elongation compared with NO-O in Rc (Figure 7A). In contrast, increasing ΔC652 levels appeared to cause increasing interference when compared with NO-O in both FRc and possibly Rc (Figure 7B). ΔN633, however, appeared to interfere specifically with hypocotyl elongation in FRc: increasing overexpression levels led to strong interference with endogenous phyA activity when compared with NO-O, whereas there was no effect on hypocotyl elongation in Rc (no interference with endogenous phyB), as shown in Figure 7C. Finally, C357-S had no effect on hypocotyl elongation in either Rc or FRc at different overexpression levels compared with NO-O (Figure 7D). All other transgenic lines were indistinguishable from the untransformed control (NO-O) in 6.0 μmol m^{-2} sec^{-1} FRc (data not shown).

One possible explanation for the dominant negative phenotype of phyB, ΔN633, and ΔC652 is that overexpression of any of these phyB derivatives causes a decrease in levels of endogenous phyA. However, using a phyA-specific MAb, we detected no differences in endogenous phyA levels between the transgenic lines and the untransformed control (NO-O), as shown in Figure 8A; this result indicates that overexpression of phyB and phyB derivatives does not interfere with endogenous phyA expression. Another possible reason for dominant interference in the case of phyB and ΔC652, which are both spectrally active, is that they sequester endogenous chromophore away from endogenous phyA. Yet hypocotyl length was not reduced in any of the transgenic lines in FRc in the presence of the exogenous chromophore precursor biliverdin, suggesting that chromophore sequestration may not be the basis for the dominant negative phenotype of phyB and ΔC652 (data not shown). However, ΔΔA measurements of dark- and Rc-grown seedlings suggested that chromophore may be limiting to endogenous phyA in seedlings overexpressing phyB and ΔC652 at very high levels, whereas no evidence of this effect was observed for ABO (data not shown).

To test one possible basis for the strong dominant negative effect of ΔN633, which is spectrally inactive and therefore not capable of chromophore sequestration, we assayed for potential heterodimerization between ΔN633 and endogenous phyA in Figure 8B. At least some of the dimerization-competent ΔN633 should be expressed in the same cells as endogenous phyA, based on analysis of expression patterns of phyA–β-glucuronidase (phyA–GUS) compared with cauliflower

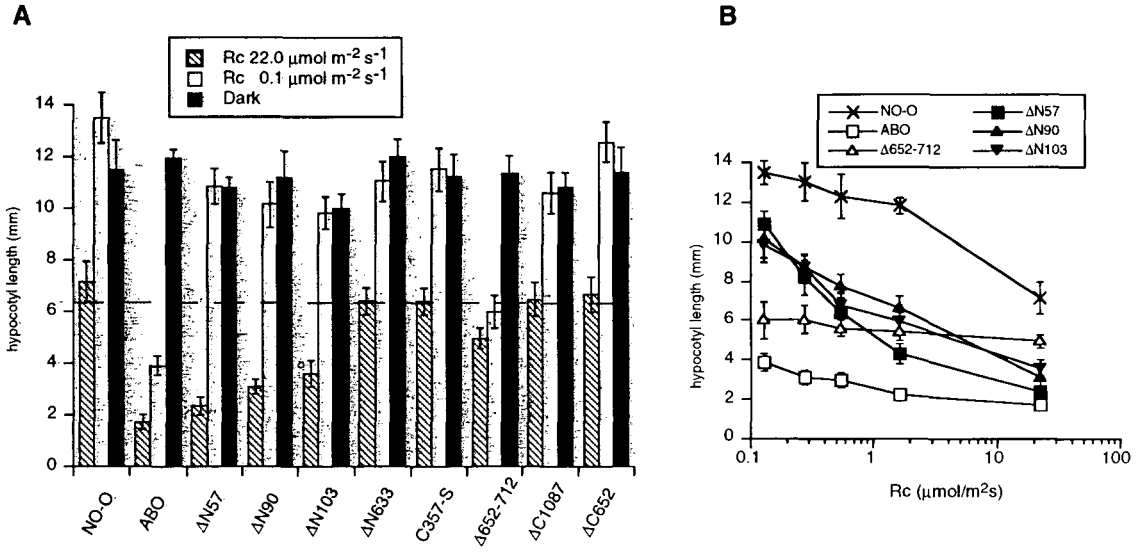

Figure 6. Differential Hypocotyl Elongation Response of Transgenic Seedlings Expressing phyB and phyB Derivatives as a Function of Fluence Rates of Rc.

(A) Hypocotyl lengths of phyB- and phyB mutant derivative–expressing transgenic lines as well as the untransformed control (NO-O) in Rc and darkness. Hypocotyl length was determined for >20 4-day-old seedlings grown in Rc of two different fluence rates (22.0 μmol m^{-2} sec^{-1} and 0.1 μmol m^{-2} sec^{-1}) or in the dark. Bars represent mean hypocotyl lengths, and each error bar represents one standard deviation. The broken line indicates the mean length of the untransformed wild type (NO-O) growing in Rc at 22 μmol m^{-2} sec^{-1} minus one standard deviation.
(B) Fluence rate response curves of selected phyB- and phyB derivative–overexpressing seedlings. The transgenic lines (listed in the insert) that showed significant reduction of hypocotyl elongation in response to Rc, compared with the untransformed wild type (NO-O) in **(A)**, were grown in a range of different Rc fluence rates (0.1 μmol m^{-2} sec^{-1} to 22.0 μmol m^{-2} sec^{-1}). Mean hypocotyl length was determined for >20 4-day-old seedlings, and each error bar denotes one standard deviation.

mosaic virus 35S–GUS fusions (Somers and Quail, 1995). After nondenaturing gel electrophoresis of ΔN633 and NO-O, we probed the right half of the immunoblot with MAb B2, which recognizes both ΔN633 and endogenous phyB, and we probed the left half with a phyA-specific MAb. No phyA-reactive band was present in the ΔN633 complex, and no reduction of homodimeric phyA levels was observed in the ΔN633 compared with the NO-O extracts, indicating that there was no detectable heterodimerization between endogenous phyA and the overexpressed phyB C-terminal derivative. Taken together, the available data suggest that ΔN633 may interfere with downstream components of phyA signaling.

DISCUSSION

N-Terminal and C-Terminal Domains of phyB Are Required Contiguously for Activity

Neither of the two structural domains of phyB are sufficient for biological activity when assayed by overexpression in transgenic Arabidopsis. The N-terminal domain of phyB (ΔC652) does not exhibit normal activity when overexpressed by itself, even though it is fully spectrally active. These findings could indicate that the N-terminal domain does not fold correctly for biological activity. Alternatively, dimerization may be required for phyB activity because this phyB derivative is monomeric. Lastly, deletion of a proposed signal transducing (regulatory) region localized on the C-terminal domain may be responsible for loss of activity in ΔC652 (Quail et al., 1995; Wagner and Quail, 1995; Wagner et al., 1996). The latter hypothesis predicts that a construct that retains this regulatory region, but deletes the remainder of the C-terminal domain (including the dimerization sites), should be biologically active. One such construct was generated for phyA but did not accumulate at high enough levels in transgenic plants to test for biological activity (Cherry et al., 1993).

Removal of the ligand binding (receptor) domain from certain biological molecules, for example, receptor kinases, results in constitutive activity of the signaling domain (Rebay et al., 1993; Struhl et al., 1993). Thus, separation of the chromophore-bearing N-terminal (light-receptor) domain from the putative signaling activity of the C-terminal domain of phyB (Wagner and Quail, 1995) might yield constitutive activity. However, overexpression of the C-terminal domain alone (ΔN633) did not result in constitutive deetiolation, even though the molecule dimerized efficiently. Insufficient folding of the C-terminal domain may be responsible for lack of biological activity. Alternatively, additional N-terminal regions may be necessary

for constitutive activity of the truncated spectrally inactive molecule. Lastly, a photoconversion-induced change in the C-terminal domain may be required for activity.

The N-terminal and C-terminal domains of phyB appear to be required for biological activity in *cis*, because plants overexpressing both ΔN633 and ΔC652 domains in *trans* are indistinguishable from NO-O (data not shown). Possible reasons for the requirement of the contiguous presence of both domains include the necessity for signal transfer from the N-terminal to the C-terminal domain of phyB before signal transfer from the C-terminal domain to the cellular interaction partner of phyB (Wagner et al., 1996).

N-Terminal Extension of phyB Is Important for Normal Signaling Rates

The N-terminal extension (amino acids 6 to 57) characteristic of phyB was found to be necessary for the full activity of phyB most evident at low fluence rate Rc. These data provide strong evidence for the functional importance of the phyB/phyD–specific N-terminal extension. The deletion does not interfere with phyB dimerization. However, the absorption maximum of the Pfr form in the far-red region of the spectrum may be altered slightly. The reduced efficiency of ΔN57 could thus be due to reduced efficiency of photoconversion or, alternatively, to a reduced signal transduction. Because the N-terminal extension deleted in ΔN57 is present in the phyB/phyD–type phytochromes but not in phyA (Clack et al., 1994), it may be important for maximal efficiency of this group of photoreceptors specifically. In addition, a deletion derivative of phyA (ΔN52), which

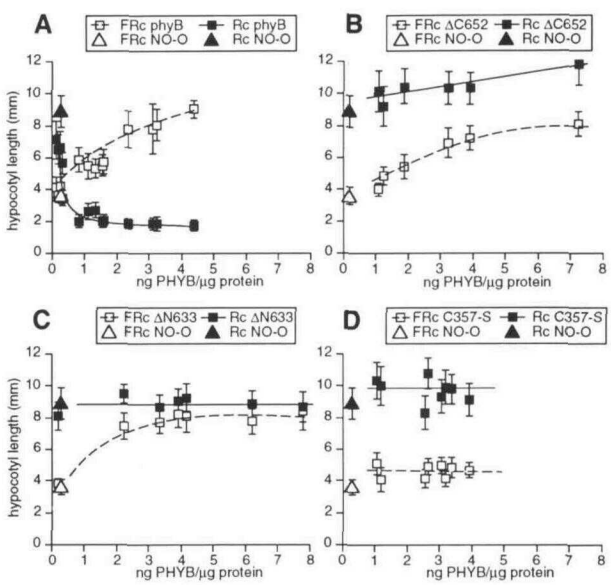

Figure 7. Hypocotyl Length in FRc as a Function of Overexpression Levels of phyB and phyB Derivatives.

Hypocotyl lengths of 4-day-old transgenic Arabidopsis seedlings overexpressing phyB and selected phyB derivatives at different levels were measured after growth in FRc (6.0 μmol m^{-2} sec^{-1}). The construct analyzed is indicated in the insert of each panel.

(A) Transgenic phyB seedlings.

(B) Transgenic ΔC652 seedlings.

(C) Transgenic ΔN633 seedlings.

(D) Transgenic C357-S seedlings.

Mean hypocotyl length in FRc is indicated and compared with that in Rc (at 22.0 μmol m^{-2} sec^{-1} as in Figure 2) for each construct. The untransformed control, NO-O, was included under both conditions. Hypocotyl length is given as a function of densitometrically determined transgene amounts (nanograms of phyB per microgram of crude protein). Each error bar denotes one standard deviation.

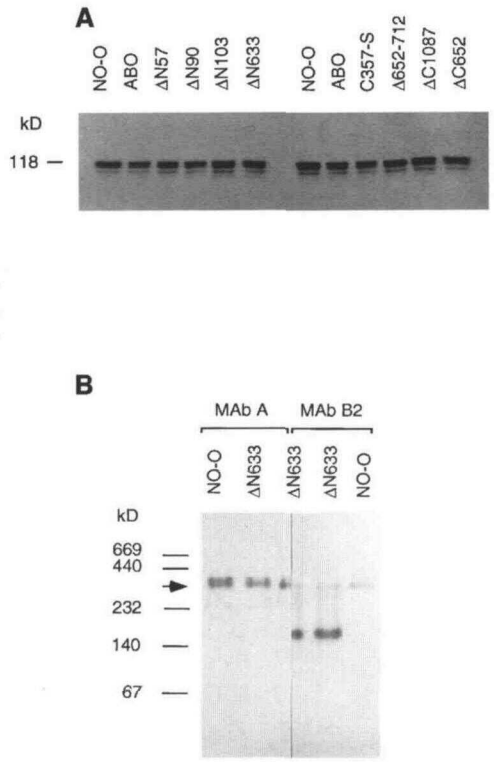

Figure 8. Analysis of phyA Levels and Dimerization.

(A) Immunoblot of endogenous phyA in transgenic lines and NO-O. Crude extracts of 7-day-old dark-grown seedlings were subjected to denaturing gel electrophoresis (6.5%), followed by immunoblotting and development with a phyA-specific MAb. Twelve micrograms of crude protein was loaded per lane. Molecular mass of phyA is indicated at left (in kilodaltons).

(B) Nondenaturing gel electrophoresis of wild-type and transgenic seedlings overexpressing the ΔN633 phyB mutant derivative. Crude extracts (14 μg of crude protein per lane) of 7-day-old dark-grown seedlings of ΔN633 and NO-O lines were subjected to nondenaturing gradient gel electrophoresis (4 to 30%). After being cut vertically in the central lane, the left half of the blot was probed with a phyA-specific MAb, whereas the right half was probed with MAb B2, which recognizes endogenous phyB as well as ΔN633. Molecular mass of nonstained markers is indicated at left (in kilodaltons). The arrow points to full-length phyB (317 kD).

is the equivalent of ΔN90 of phyB, was found to show dominant negative interference in FRc but not in Rc (Boylan et al., 1994), indicating the importance of the deleted sequence to phyA activity specifically in FRc. Moreover, photosensory specificity of phyA and phyB has been mapped to the N-terminal domain of both photoreceptors (Wagner et al., 1996). Thus, the N-terminal extension of phyB is a good candidate for a region required for phyB-specific activity.

A Small Central Region May Be Important for Signal Transfer of phyB and phyA

A small region (amino acids 652 to 712) at the N-terminal end of the C-terminal domain was found to be important for maximal activity of phyB. The Δ652-712 polypeptide is spectrally intact and therefore most likely unaffected in photosignal perception and photoconversion. It is also apparently dimeric, although some perturbation of dimerization properties or aggregation of this protein in the cell cannot be excluded. ΔC617-712 retains high sensitivity to low fluence rate Rc, but it shows saturation in high fluence rates of Rc at a response level much below that seen in seedlings overexpressing phyB. This unique fluence rate response pattern indicates a reduction of maximal activity per mole of ΔC617-712 that cannot be compensated for by higher rates of photoexcitation. Thus, this construct is most likely affected in a process downstream of signal perception and intramolecular processing, such as reduction in the maximal capacity for signal transfer to downstream components. Recent point mutational analysis of phyB has also identified a small C-terminal domain region adjacent to that deleted in Δ652-712 as being important for phyB regulatory activity (Wagner and Quail, 1995). The Δ652-712 construct deletes the first of two repeat sequences of unknown function recently noted by Jones and Edgerton (1994). Deletions such as in Δ652-712 could impact proper folding of the protein. However, Δ652-712 is almost as active as phyB at low fluence rates (high sensitivity to Rc), suggesting that the reduction in activity per mole phyB may not be due to gross structural aberration.

Several lines of evidence indicate that this central region is also important for phyA activity. A deletion construct similar to Δ652-712 was generated for transgenic phyA (Δ617-686; Boylan et al., 1994) and resulted in loss of normal transgene-encoded phyA activity. Mutational analysis of phyA identified a region overlapping with both the region deleted in Δ652-712 and the region identified for phyB (Wagner and Quail, 1995) as important for phyA regulatory activity (Quail et al., 1995; Xu et al., 1995). Lastly, analysis of chimeric phyA–phyB constructs has shown that the phyB C-terminal domain can functionally replace the phyA C-terminal domain and vice versa (Wagner et al., 1996), indicating that in the context of the full-length molecule, the C-terminal domain is functionally equivalent in both photoreceptors. Taken together, these data strongly suggest that the small region at the N-terminal end of the C-terminal domain is important for the regulatory activity of both phyA and phyB. The data also are consistent with the possibility that there is a similar mechanism of downstream signal transfer for both photoreceptors.

phyB Interferes with the Activity of Endogenous phyA

One unexpected finding was that full-length Arabidopsis phyB as well as both halves of the phyB molecule interfere with endogenous phyA activity in FRc. This dominant negative effect (Herskowitz, 1987) is readily observable in low-intensity FRc (limiting light signal).

Photoconversion appears to be important for interference by full-length phyB because the spectrally inactive C357-S construct does not cause a dominant negative phenotype. Previously, an ethyl methane sulfonate–mutagenized ABO line carrying a mutant transgene-encoded phyB was identified. This mutant shows 100-fold greater spectral activity than endogenous phyB yet does not interfere with phyA activity (Wagner and Quail, 1995). The point mutation in this line occurs in the proposed C-terminal domain regulatory region and causes strong reduction of activity in Rc (Wagner and Quail, 1995). The most likely interpretation of these data is that the mutated residue in the small (regulatory) region on the C-terminal domain of phyB is not only important for activity in Rc but is also necessary for the interference of phyB with phyA activity. It cannot be ruled out, however, that at least part of the dominant negative effect of phyB overexpression is due to chromophore sequestration, as discussed for ΔC652 below.

Because both ΔN633 and ΔC652 interfere with phyA activity, the 20 amino acids (633 to 652) common to both constructs could be the region involved in dominant negative interference. The overlap is adjacent to the deletion found to be important in phyB activity (652 to 712). Alternatively, uncoupling of the two major domains may result in an activity for each domain different from that observed in the context of the full-length molecule. Lastly, interference from each construct may be caused by a different mechanism.

Deletion of the signaling portion of receptor molecules often leads to dominant negative phenotypes (Rebay et al., 1993). Overexpression of phyB (ΔC652) or phyA (ΔC617) constructs, in which the entire C-terminal domain is deleted, causes a dominant negative effect in Rc and FRc (this study; Boylan et al., 1994). The dominant negative effect of ΔC652 is caused by neither cosuppression nor formation of nonproductive heterodimers (they are monomeric). We cannot rule out the possibility that the dominant negative interference of ΔC652 may be due to sequestration of chromophore away from endogenous phytochromes, reducing the latter's activity. Alternatively, deletion of the C-terminal domain might cause dominant negative effects by nonproductive interaction of the N-terminal domain with a phyA/phyB interaction partner. If so, this interpretation would suggest the presence of a regulatory element important for phyB and phyA function between amino acids 103 and 652 of phyB, as proposed previously (Boylan et al., 1994).

ΔN633 causes a very strong dominant negative phenotype in FRc. This effect is not due to chromophore sequestration. We can also rule out cosuppression of or heterodimerization with endogenous phyA. It appears most likely, therefore, that ΔN633 interferes with phyA signal transduction by nonproductive interaction with endogenous signaling components, possibly via the activity of the proposed regulatory region at the N-terminal end of the C-terminal domain common to both photoreceptors. This regulatory region may be exposed in the ΔN633 molecule but buried in C357-S, which is also spectrally inactive but does not show dominant negative interference. Previous data indeed suggest that in the context of the full-length molecule, this region is susceptible to proteolysis in the Pfr form only (Lagarias and Mercurio, 1985; Grimm et al., 1988). Thus, phyB and phyA may share signal transduction pathway components.

Because the regulatory region at the N-terminal end of the C-terminal domain appears to be important for both phyA and phyB signal transduction (this study; Boylan et al., 1994; Wagner and Quail, 1995; Xu et al., 1995; Wagner et al., 1996), it is surprising that ΔN633 causes dominant negative interference with phyA but not with phyB activity. The reason for this is not understood. The small regulatory region on the C-terminal domain of phyB may exhibit a much higher affinity for the putative interaction partner than the equivalent phyA region, thus drawing the interaction partner away from phyA but not from phyB. Alternatively, endogenous phyB may have a mechanism for protection against dominant negative interference involving this region, like transient binding to the putative common reaction partner in Rc (Cherry et al., 1993).

In sum, we have identified two small regions of phyB that are important for efficient signaling rates. One (N-terminal) region appears to be important specifically for phyB signal perception or transduction. It will be interesting to determine whether this region is sufficient to direct phyB specificity in the context of a different full-length phytochrome. The second (central) region is possibly involved in both phyB and phyA signal transduction. Future characterization of these regions will no doubt help to identify the phyB and/or phyA interaction partners.

METHODS

Construction, Cloning, and Transformation of Phytochrome B Derivatives

Eight phytochrome B (phyB) deletion and point mutation derivatives were generated for overexpression in transgenic Arabidopsis (Figure 1). First, three subclones of full-length phyB in pBAB (pBSK+; Stratagene) were generated: pBSKI (NdeI-SpeI), pBSKII (BglII-PstI), and pBKSIII (SpeI-BamHI). Polymerase chain reaction (PCR)–generated sequences and cloning sites were confirmed by sequencing. The three N-terminal deletions of phyB were constructed by using PCR. The 5′ end of the forward PCR primer for all three constructs contained NdeI and XbaI sites for cloning, followed by noncomplementary codons for the first five amino acids of full-length phyB (methionine, valine, serine, glycine, and valine) and by seven codons complementary to amino acids 58 to 64 for construct ΔN57, to amino acids 91 to 97 for construct ΔN90, and to amino acids 104 to 110 for construct ΔN103. The PCR products were first subcloned into pBSKI (NdeI-BglII), followed by fusion of a ClaI-MluI fragment to pMAB316 (Wagner et al., 1991). ΔN633 was created by using the same procedure, except that the forward primer annealed to codons for amino acids 633 to 639. The PCR product was subcloned into pBAB (XbaI-SpeI), followed by fusion to the remainder of phyB in pMAB316 as a ClaI-PpuMI fragment. The single amino acid change of cysteine 357 to serine was created by oligonucleotide mutagenesis (Kunkel, 1985) (TGT was mutated to TCT at position 1079).

The internal deletion in Δ652-712 was created after two PCR reactions. The reverse primer of the first PCR reaction annealed to nucleotides 1936 to 1956 and created a HpaI site between nucleotides 1954 and 1959. This PCR product was digested with NcoI and HpaI. The second PCR reaction used a forward primer complementary to nucleotides 2136 to 2156, except a silent T-to-C change was introduced at position 2138 to create a HpaI site between nucleotides 2133 and 2138. This PCR product was digested with HpaI and SpeI. The two PCR fragments were subcloned into pBSKII (NcoI-SpeI) and moved into pMAB316 digested with MluI and PpuMI. The C-terminal deletion of ΔC1087 was introduced by digesting pBKSIII with PpuMI and EcoRI (which also cuts in the polylinker), followed by ligation with pMAB316 digested with the same two enzymes. This deletes the C-terminal 88 amino acids and introduces 11 new amino acids (vector in frame) before terminating. ΔN633 was generated by digestion of the Δ652-712 phyB derivative with MluI and HpaI, followed by subcloning as MluI/EcoRV into pBAB. A MluI-EcoRI fragment was then cloned into the ΔC1087 derivative of pMAB316. All constructs retained the same 5′ untranslated leader to cauliflower mosaic virus 35S promoter fusion as described for phyB (Wagner et al., 1991) and were transformed into Arabidopsis ecotype NO-O (Nössen), as described previously (Wagner et al., 1991).

Plant Growth, Hypocotyl Measurements, and Light Sources

For hypocotyl measurements, seeds were treated as described by Wagner and Quail (1995). Seedling growth (hypocotyl elongation) was performed in different light regimes (continuous red and far-red light [Rc and FRc], continuous white light, and dark) for 3 days. For hypocotyl-length determination, seedlings were laid flat on agar plates and photographed. The resulting slides were projected onto a digitizing tablet, traced, and measured using National Institutes of Health image software (public domain; Bethesda, MD). The light sources and photometer used were described previously (Wagner et al., 1991). For lower fluence rates, neutral density filters were constructed from white paper and developed using XOMAT autoradiograph film (Kodak, Rochester, NY).

Tissue Extraction and Spectral Analysis

For tissue extraction, seedlings were grown as described above except that growth in the different light regimes was allowed for 6 days to maximize tissue yield. Crude extracts for denaturing and nondenaturing electrophoresis as well as concentrated extracts for spectral analyses were prepared essentially as previously described by Wagner and Quail (1995). However, the tissue for concentrated extracts was ground in liquid nitrogen and rapidly resuspended in extraction buffer,

which significantly increased the yield per gram fresh weight. The instrumentation used for spectral analysis was described by Wagner et al. (1991).

Denaturing and Nondenaturing Electrophoresis, Immunoblotting, and Antibodies

Denaturing electrophoresis was performed as described previously by Wagner et al. (1991). For the nondenaturing 4 to 30% gradient electrophoresis, the resolving gel consisted of 4% acrylamide, 59 mM Tris, pH 8.0, and 30% acrylamide. The stacking gel consisted of 4% acrylamide and 79 mM Tris, pH 8.0. The running buffer used was 250 mM Tris and 1.9 M glycine, pH 8.6. The sample buffer contained 40% sucrose and 100 mM Tris, pH 8.0, and 0.005% bromophenol blue. The gel was run to equilibrium (>16 hr at 150 V) at 4°C. Transfer of both gel types was performed for 2 hr at 700 mA in 20% methanol, 150 mM glycine, and 25 mM Tris, pH 8.6. The antibody-staining procedure was described by Wagner et al. (1991). Epitopes of the phyB-selective monoclonal antibodies (MAbs) raised against rice (Wagner et al., 1991) and Arabidopsis (Somers et al., 1991) phyB were first mapped to the N-terminal or C-terminal domain of phyB, using crude extracts of seedlings overexpressing ΔC652 and ΔN633, respectively. MAb B1 recognized the N-terminal domain of phyB. It also recognized the ΔN90 deletion construct but reacted only weakly with ΔN103, indicating that it recognizes an epitope near amino acids 90 and 103. MAb B2, by contrast, recognized the C-terminal domain yet failed to recognize the Δ652-712 construct. Therefore, it recognizes an epitope between amino acids 652 and 712 of phyB. The phyA-specific MAb, which reacts with endogenous Arabidopsis phyA, was described by Boylan and Quail (1991).

Densitometric and Spectrophotometric Quantification of phyB

For densitometric quantitation of the phyB overexpression levels, crude extracts were prepared from phyB, C357-S, ΔN633, ΔC652, ABO, and NO-O. All extracts were then diluted to approximately the same concentration of overexpressed protein. Three serial twofold dilutions of ABO were loaded, followed by the same three dilutions of extracts from five different transgenic lines, and a repeat of two ABO concentrations was loaded on each gel. Each immunoblot was stained and analyzed individually, and protein concentrations were calculated by using ABO as a reference. After video imaging, the intensity of each band was analyzed using National Institutes of Health image software. Spectral quantitation (ΔΔA measurements) was performed by using 10-fold concentrated extracts as described above.

ACKNOWLEDGMENTS

This article is dedicated to Dr. Pill Soon Song on his 60th birthday. We thank Nancy Douglas for help with the transgenic work, Jim Tepperman for assistance with the antibody production, Dave Somers for phyB-selective MAbs to screen for differential epitope detection, Jennifer Fletcher and John Wagner for critical reading of the manuscript, Craig Fairchild and John Wagner for useful discussion, and David Hantz for excellent greenhouse care of our plants. This work was supported by Department of Energy Office of Basic Energy Grant No. FG03-92 ER 13742 and U.S. Department of Agriculture Agricultural Research Service Current Research Information Service Grant No. 5335-21000-006-00D.

Received November 9, 1995; accepted March 11, 1996.

REFERENCES

Boylan, M.T., and Quail, P.H. (1989). Oat phytochrome is biologically active in transgenic tomatoes. Plant Cell **1,** 765–773.

Boylan, M.T., and Quail, P.H. (1991). Phytochrome A overexpression inhibits hypocotyl elongation in transgenic Arabidopsis. Proc. Natl. Acad. Sci. USA **88,** 10806–10810.

Boylan, M., Douglas, N., and Quail, P.H. (1994). Dominant negative suppression of Arabidopsis photoresponses by mutant phytochrome A sequences identifies spatially discrete regulatory domains in the photoreceptor. Plant Cell **6,** 449–460.

Cherry, J.R., Hershey, H.P., and Vierstra, R.D. (1991). Characterization of tobacco expressing functional oat phytochrome—Domains responsible for the rapid degradation of Pfr are conserved between monocots and dicots. Plant Physiol. **96,** 775–785.

Cherry, J.R., Hondred, D., Walker, J.M., and Vierstra, R.D. (1992). Phytochrome requires the 6-kDa N-terminal domain for full biological activity. Proc. Natl. Acad. Sci. USA **89,** 5039–5043.

Cherry, J.R., Hondred, D., Walker, J.M., Keller, J.M., Hershey, H.P., and Vierstra, R.D. (1993). Carboxy-terminal deletion analysis of oat phytochrome A reveals the presence of separate domains required for structure and biological activity. Plant Cell **5,** 565–575.

Clack, T., Mathews, S., and Sharrock, R.A. (1994). The phytochrome apoprotein family in Arabidopsis is encoded by five genes—The sequences and expression of phyD and phyE. Plant Mol. Biol. **25,** 413–427.

Dehesh, K., Tepperman, J., Christensen, A.H., and Quail, P.H. (1991). *phyB* is evolutionarily conserved and constitutively expressed in rice seedling shoots. Mol. Gen. Genet. **225,** 305–313.

Dehesh, K., Franci, C., Parks, B.M., Seeley, K.A., Short, T.W., Tepperman, J.M., and Quail, P.H. (1993). Arabidopsis *HY8* locus encodes phytochrome A. Plant Cell **5,** 1081–1088.

Edgerton, M.D., and Jones, A.M. (1992). Localization of protein–protein interactions between subunits of phytochrome. Plant Cell **4,** 161–171.

Edgerton, M.D., and Jones, A.M. (1993). Subunit interactions in the carboxy-terminal domain of phytochrome. Biochemistry **32,** 8239–8245.

Grimm, R., Eckerskorn, C., Lottspeich, F., Zenger, C., and Rüdiger, W. (1988). Sequence analysis of proteolytic fragments of 124-kilodalton phytochrome from etiolated *Avena sativa* L.: Conclusions on the conformation of the native protein. Planta **174,** 396–401.

Herskowitz, I. (1987). Functional inactivation of genes by dominant negative mutations. Nature **329,** 219–222.

Jones, A.M., and Edgerton, M.D. (1994). The anatomy of phytochrome, a unique photoreceptor in plants. Semin. Cell Biol. **5,** 295–302.

Jones, A.M., Allen, C.D., Gardner, G., and Quail, P.H. (1986). Synthesis of phytochrome apoprotein and chromophore are not coupled obligatorily. Plant Physiol. **81,** 1014–1016.

Kay, S.A., Nagatani, A., Keith, B., Deak, M., Furuya, M., and Chua, N.-H. (1989). Rice phytochrome is biologically active in transgenic tobacco. Plant Cell **1,** 775–782.

Keller, J., Shanklin, J., Vierstra, R.D., and Hershey, H.P. (1989). Expression of a functional monocotyledonous phytochrome in transgenic tobacco. EMBO J. **8,** 1005–1012.

Kunkel, T.A. (1985). Rapid and efficient site-specific mutagenesis without phenotypic selection. Proc. Natl. Acad. Sci. USA **82,** 488–492.

Lagarias, J.C., and Mercurio, F.M. (1985). Structure function studies on phytochrome. Identification of light induced conformational changes in 124 kDa *Avena* phytochrome *in vitro*. J. Biol. Chem. **260,** 2415–2423.

McCormac, A.C., Wagner, D., Boylan, M.T., Quail, P.H., and Smith, H. (1993). Photoresponses of transgenic Arabidopsis seedlings expressing introduced phytochrome-B encoding cDNAs: Evidence that phytochrome A and phytochrome B have distinct photoregulatory functions. Plant J. **4,** 19–27.

Nagatani, A., Chory, J., and Furuya, M. (1991). Phytochrome B is not detectable in the *hy3* mutant of *Arabidopsis*, which is deficient in responding to end-of-day far-red light treatments. Plant Cell Physiol. **32,** 1119–1122.

Nagatani, A., Reed, J.W., and Chory, J. (1993). Isolation and initial characterization of Arabidopsis mutants that are deficient in phytochrome A. Plant Physiol. **102,** 269–277.

Parks, B.M., and Quail, P.H. (1993). *hy8*, a new class of Arabidopsis long hypocotyl mutants deficient in functional phytochrome A. Plant Cell **5,** 39–48.

Quail, P.H. (1991). Phytochrome: A light-activated molecular switch that regulates plant gene expression. Annu. Rev. Genet. **25,** 389–409.

Quail, P.H. (1994). Phytochrome genes and their expression. In Photomorphogenesis in Plants, 2nd ed, R.E. Kendrick and G.H.M. Kronenberg, eds (Dordrecht, The Netherlands: Kluwer), pp. 71–104.

Quail, P.H., Boylan, M.T., Parks, B.M., Short, T.W., Xu, Y., and Wagner, D. (1995). Phytochromes: Photosensory perception and signal transduction. Science **268,** 675–680.

Rebay, I., Fehon, R.G., and Artavanis-Tsakonas, S. (1993). Specific truncations of Drosophila Notch define dominant activated and dominant negative forms of the receptor. Cell **74,** 319–329.

Reed, J.W., Nagpal, P., Poole, D.S., Furuya, M., and Chory, J. (1993). Mutations in the gene for the red/far-red light receptor phytochrome B alter cell elongation and physiological responses throughout Arabidopsis development. Plant Cell **5,** 147–157.

Sharrock, R.A., and Quail, P.H. (1989). Novel phytochrome sequences in *Arabidopsis thaliana*: Structure, evolution, and differential expression of a plant regulatory photoreceptor family. Genes Dev. **3,** 1745–1757.

Somers, D.E., and Quail, P.H. (1995). Temporal and spatial expression patterns of *PHYA* and *PHYB* genes in Arabidopsis. Plant J. **7,** 413–427.

Somers, D.E., Sharrock, R.A., Tepperman, J.M., and Quail, P.H. (1991). The *hy3* long hypocotyl mutant of Arabidopsis is deficient in phytochrome B. Plant Cell **3,** 1263–1274.

Stockhaus, J., Nagatani, A., Halfter, U., Kay, S., Furuya, M., and Chua, N.-H. (1992). Serine-to-alanine substitutions at the amino-terminal region of phytochrome A result in an increase in biological activity. Genes Dev. **6,** 2364–2372.

Struhl, G., Fitzgerald, K., and Greenwald, I. (1993). Intrinsic activity of the Lin-12 and Notch intracellular domains in vivo. Cell **74,** 331–345.

Vierstra, R.D., and Quail, P.H. (1986). Phytochrome: The protein. In Photomorphogenesis in Plants, R.E. Kendrick and G.H.M. Kronenberg, eds (Dordrecht, The Netherlands: Martinus Nijhoff), pp. 35–60.

Vierstra, R.D., Quail, P.H., Hahn, T.R., and Song, P.S. (1987). Comparison of the protein conformations between different forms (Pr and Pfr) of native (124 kDa) and degraded (118/114 kDa) phytochromes from *Avena sativa*. Photochem. Photobiol. **45,** 429–432.

Wagner, D., and Quail, P.H. (1995). Mutational analysis of phytochrome B identifies a small COOH terminal-domain region critical for regulatory activity. Proc. Natl. Acad. Sci. USA **92,** 8596–8600.

Wagner, D., Tepperman, J.M., and Quail, P.H. (1991). Overexpression of phytochrome B induces a short hypocotyl phenotype in transgenic Arabidopsis. Plant Cell **3,** 1275–1288.

Wagner, D., Fairchild, C.D., Kuhn, R.M., and Quail, P.H. (1996). Chromophore-bearing NH_2-terminal domains of phytochromes A and B determine their photosensory specificity and differential light lability. Proc. Natl. Acad. Sci. USA, in press.

Whitelam, G.C., Johnson, E., Peng, J., Carol, P., Anderson, M.L., Cowl, J.S., and Harberd, N.P. (1993). Phytochrome A null mutants of Arabidopsis display a wild-type phenotype in white light. Plant Cell **5,** 757–768.

Xu, Y., Parks, B.M., Short, T.W., and Quail, P.H. (1995). Missense mutations define a restricted segment in the C-terminal domain of phytochrome A critical to its regulatory activity. Plant Cell **7,** 1433–1443.